

Structure and Bonding of the Polytopic Molecule Li[BO]. A Theoretical Investigation

Aristotle Papakondylis and Aristides Mavridis*

Laboratory of Physical Chemistry, Department of Chemistry, National and Kapodistrian University of Athens, P.O. Box 64004, 157 10 Zografou, Athens, Greece

Received: March 5, 2001; In Final Form: May 11, 2001

The potential energy surface of the reaction $\text{Li}({}^2\text{S}/{}^2\text{P}) + \text{BO}({}^2\text{X}\Sigma^+)$ was investigated theoretically using multireference variational methods in conjunction with flexible correlation consistent basis sets. On the ground-state singlet surface ($\tilde{\chi}^1\text{A}'$), three practically degenerate minima were detected, two linear Li–BO and Li–OB ($\text{X}^1\Sigma^+$) and one bent Li–OB ($\tilde{\chi}^1\text{A}'$), the latter formally being the global one. An energy barrier of about 10 kcal/mol was found to separate the two linear configurations. Potential energy curves of excited singlet and triplet linear states were also examined. The involvement of the ionic interacting fragments $\text{Li}^+({}^1\text{S}) + \text{BO}^-({}^1\text{X}\Sigma^+)$ seems to affect all states via avoided crossings, giving rise to highly ionic equilibrium states, particularly in the Li–OB isomer. As a result, the Li atom rotates freely around the O-site of BO moiety within a LiOB angle from 100° to 180° .

1. Introduction

The BO molecule ($\text{X}^2\Sigma^+$) is known to interact with a variety of radicals,¹ forming molecular systems which have been characterized as polytopic, meaning that they feature multiple, energetically close, isomers.² In our recent study of the cation ScBO^+ ,¹ three minima have been detected on the ground-state potential energy surface (PES), two linear $\text{Sc}-\text{BO}^+$ and $\text{Sc}-\text{OB}^+$ ($\text{X}^2\Delta$) and one bent $\text{Sc}-\text{OB}^+$ ($\tilde{\chi}^2\text{A}''$), the last being the global one. An analogous situation seems to hold for the Li[BO] system which exhibits also three minima on its ground PES, two linear and one bent.^{2,3}

The literature on the Li[BO] system is very limited. First, Nemukhin et al.² and later Nemukhin and Stepanov,⁴ using SCF, CASSCF/DZ+P, and CASSCF + limited CISD/DZ+P methods, respectively, concluded that the Li[BO] molecule shows polytopic behavior and that the (linear) Li–BO isomer is more stable than the (linear) Li–OB by about 4 kcal/mol.⁴ Recently, Fuentealba,⁵ using G2MP2 and B3LYP/6-311G** methods, came to the conclusion that all three isomers, the two linear (Li–BO and Li–OB) and one bent Li–OB, are essentially isoenergetic within the accuracy of his calculations. Finally, the experimental investigation of the reaction $\text{Li}(\text{g}) + \text{BO}(\text{g}) \rightarrow \text{Li}[\text{BO}](\text{g})$ by Knudsen effusion mass spectrometry³ seems to favor the linear Li–OB more than the linear Li–BO by 4 ± 1 kcal/mol.

In an effort to clarify the Li + BO interaction and, perhaps, to give a definitive answer on the details of the Li[BO] PES and bonding mechanisms, we have performed large-scale variational multireference calculations, coupled with quantitative correlation-consistent basis sets. In particular, we have examined the singlet and triplet potential energy surfaces of the reaction $\text{Li}({}^2\text{S}/{}^2\text{P}) + \text{BO}({}^2\text{X}\Sigma^+)$ and the role of the ionic interaction $\text{Li}^+({}^1\text{S}) + \text{BO}^-({}^1\text{X}\Sigma^+)$.

2. Methods

For the Li, B, and O atoms, the correlation-consistent quadruple- ζ quality basis sets of Dunning^{6a} were employed but with the functions of g angular momentum removed, cc-

pVQZ-g. To obtain a reasonable description of the BO^- anion (vide infra), we augmented the B and O atomic sets by a complete set of diffuse functions, resulting to the aug-cc-pVQZ-g basis set.^{6b} Our final, generally contracted one-electron space, $[(6s5p4d3f)_{\text{B},\text{O}}/(5s4p3d2f)_{\text{Li}}]$, numbers 170 spherical Gaussian functions.

In a complete (valence) active space SCF (CASSCF) description, the 10 active electrons ($1(\text{Li}) + 3(\text{B}) + 6(\text{O})$) should be allowed to occupy a 12-orbital space, CASSCF(10/12). Such an allotment produces under C_s symmetry restrictions about 85 000 (singlets) or 142 000 (triplets) configuration functions (CF), rendering subsequent configuration interaction (CI) calculations out of this space impractical. Instead, a CASSCF wave function was constructed by distributing two electrons only, the 2s on Li and 5σ on BO ($\text{X}^2\Sigma^+ = 1\sigma^2 2\sigma^2 3\sigma^2 4\sigma^2 5\sigma^1 \pi_x^2 \pi_y^2$), among five orbitals, the four (valence) Li orbitals + the singly occupied 5σ MO of BO. This CASSCF scheme gives rise to a $11\text{A}', 4\text{A}''$ singlet or $6\text{A}'$, and $4\text{A}''$ triplet configurational space, ensuring correct asymptotic description (size consistency), i.e., $\text{Li}({}^2\text{S}/{}^2\text{P}) + \text{BO}({}^2\text{X}\Sigma^+)$ or $\text{Li}^+({}^1\text{S}) + \text{BO}^-({}^1\text{X}\Sigma^+)$ fragments. All our CASSCF calculations were state averaged⁷ over the $4\text{A}'+1\text{A}''$ states, corresponding to one Π and three Σ^+ states of the linear geometries. Valence “dynamical” correlation was obtained by single and double excitations of the 10 valence electrons out of this space (CASSCF+1+2 = MRCI), keeping the core $\sim 1s^2(\text{Li/B/O})$ electrons always doubly occupied and applying at the same time the internal contraction approach,⁸ referred to as MRCI(2/5).

All equilibrium structures thus obtained were recalculated employing MRCI calculations out of the “large” 10/12 (CASSCF-(10/12)) multireference space, but truncated according to the criterion $\sum_i C_i^2 = 0.999$, where $\{C_i\}$ are variational CASSCF coefficients. This reduces the number of CASSCF(10/12) CFs to about 1000, accompanied by CASSCF energy losses of less than 2 mhartrees as compared to the complete CASSCF(10/12) calculations. The corresponding MRCI “2/5” and “10/12” (truncated CASSCF(10/12)) expansions contain about 1.25×10^6 and 105×10^6 CFs for the singlets and 2.9×10^6 and 432×10^6 CFs for the corresponding triplets, respectively. These

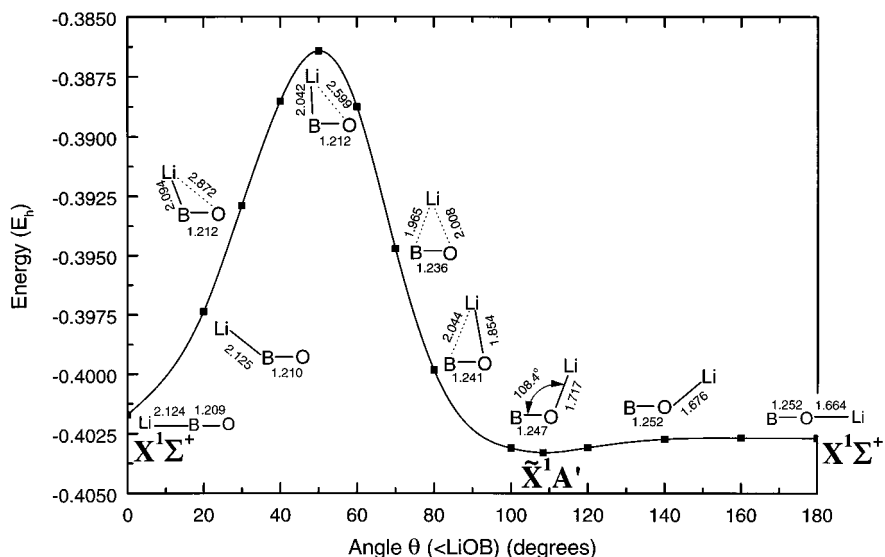


Figure 1. Minimum MRCI(2/5) energy profile of the rearrangement $\text{Li}-\text{BO}(\text{X}^1\Sigma^+)$ \rightarrow bent $\text{Li}-\text{OB}(\tilde{\text{X}}^1\text{A}')$ \rightarrow $\text{Li}-\text{OB}(\text{X}^1\Sigma^+)$; bond lengths are in Å.

TABLE 1: Total Energies E (hartree), Bond Distances r_e (Å), Dissociation Energies D_e (kcal/mol), Mulliken Charges q_0 , Dipole Moments μ (Debye), and Adiabatic Electron Affinities EA (eV) of the $\text{X}^2\Sigma^+$ State of BO in Different Methods

method	$-E$	r_e	D_e	q_0	μ	EA ^a
CISD	99.85903	1.196	170.1	-0.35	2.47	2.24
CISD+Q ^b	99.8841	—	178.0	—	—	2.42
MRCI(9/8) ^c	99.88324	1.211	191.0	-0.37	2.29	2.16 ^d
MRCI(9/8)+Q ^e	99.8927	—	190.0	—	—	2.35
t-MRCI(9/8) ^f	99.88211	1.211	190.4	-0.37	2.31	2.17
CCSD(T) ^g	99.91213	1.2079	193.4	—	—	2.50
expt	—	1.2049 ^h	193.6 ⁱ	—	—	2.508 ± 0.008 ^j

^a $EA(\text{X}) = E(\text{X}) - E(\text{X}^-)$. ^b CISD+Davidson correction. ^c Internally contracted MRCI out of $9e^-/8$ orbital CASSCF reference. ^d Obtained from a MRCI(10/8) BO^- calculation; at this level, $r_e(\text{BO}^-;\text{X}^1\Sigma^+) = 1.244 \text{ \AA}$. ^e MRCI+multireference Davidson correction, ref 14. ^f Truncated MRCI, see text. ^g Ref 13; doubly aug-cc-pV6Z basis; $r_e(\text{BO}^-;\text{X}^1\Sigma^+) = 1.240 \text{ \AA}$. ^h Ref 15. ⁱ Ref 16; $D_e = D_0 + \omega/\sqrt{2}$. ^j Ref 12.

spaces are further reduced to 0.25×10^6 and 4.5×10^6 CFs (singlets) and 0.6×10^6 and 12.7×10^6 CFs (triplets) by applying the internally contracted MRCI philosophy,⁸ referred thereafter as t-MRCI(10/12). Finally, all geometry optimizations were done at the MRCI(2/5) level using numerical gradients.

All our computations were performed by the MOLPRO96⁹ program.

3. The Li and BO Fragments

The SCF energy of the ground ${}^2\text{S}$ of Li, $E = -7.43270 E_{\text{h}}$, is in practical agreement with the numerical Hartree–Fock value of $-7.43272 E_{\text{h}}$.¹⁰ Also, the calculated ${}^2\text{P} \leftarrow {}^2\text{S}$ excitation and ionization ($\text{Li} \rightarrow \text{Li}^+ + \text{e}^-$) energies, 1.841 and 5.342 eV, are in harmony with the experimental values,¹¹ 1.848 and 5.390 eV, respectively.

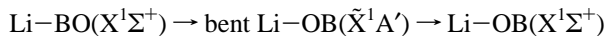
Concerning now the $\text{BO}(\text{X}^2\Sigma^+)$ radical, related structural properties at the CI and MRCI levels are listed in Table 1. The agreement with experimental values can be considered as fair; the discrepancy in the D_e at the CISD level is expected and is due, primarily, to the size nonextensivity of the CISD method. Note that results obtained with the (truncated) t-MRCI(9/8) technique compare well with the (complete) MRCI(9/8) values. Our computed (adiabatic) electron affinities (EA) of $\text{BO}(\text{X}^2\Sigma^+)$

are in acceptable agreement with the most recent experimental value of $2.508 \pm 0.008 \text{ eV}$.¹² The best theoretical EA(BO) value so far is that of Papakondylis and Mavridis,¹³ who obtained $EA(\text{BO}) = 2.50 \text{ eV}$ at the CCSD(T)/doubly aug-cc-pV6Z level of theory. We believe that the overall description of the BO and BO^- entities is adequate, since the purpose of the present study is not the accurate characterization of these species but their interaction with the Li atom.

4. Results and Discussion

We can envisage the Li atom approaching the $\text{BO}(\text{X}^2\Sigma^+)$ moiety from either end in a linear fashion, or laterally resulting to singlets or triplets.

4.1 Singlets. Figure 1 presents a minimum-energy profile of the isomerization process



at the MRCI(2/5) level of theory. The curve was constructed by optimizing all bond distances involved for every selected angle value θ ($=\angle \text{LiOB}$). Linear geometries $\text{Li}-\text{BO}$ and $\text{Li}-\text{OB}$ correspond to $\theta = 0^\circ$ and 180° , respectively. As can be seen, three minima were found, two linear and one bent, the latter formally being the global one. As Table 2 shows, the energy difference $\Delta E[\text{MRCI}(2/5)] = E(\text{Li-OB}) - E(\text{Li-BO})$ is -0.6 kcal/mol , or $\Delta E[\text{t-MRCI}(10/12)/\text{MRCI}(2/5)] = +0.5 \text{ kcal/mol}$, so the two linear isomers are degenerate within the accuracy of our methods. On the other hand, the bent $\tilde{\text{X}}^1\text{A}'$ state is $0.5-1.0 \text{ kcal/mol}$ lower in energy than the linear isomers (Table 2). Therefore, we are dealing with a genuine polytopic system and a very floppy (bent) $\text{Li}-\text{OB}$ ($\tilde{\text{X}}^1\text{A}'$) isomer with respect to the linear $\text{Li}-\text{OB}$ $\text{X}^1\Sigma^+$ state with an insignificant barrier between them. For the rearrangement $\text{Li}-\text{OB} \rightarrow \text{Li}-\text{BO}$ an energy barrier of 10.5 kcal/mol is obtained (Figure 1), as compared to an experimental thermochemical value of about 19 kcal/mol .³

Figures 2 and 3 present potential energy curves (PEC) of singlets (and triplets) of the interaction $\text{BO} + \text{Li}$ in a linear fashion at the MRCI(2/5) level of theory. All curves were constructed by keeping the geometrical parameters fixed at their equilibrium values but the relative $\text{Li}-\text{BO}$ or $\text{Li}-\text{OB}$ distance.

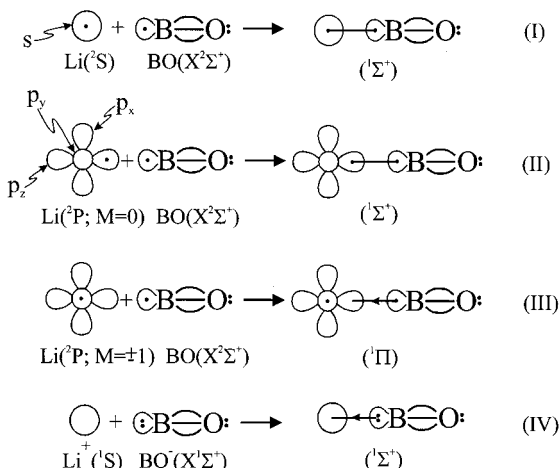
Li-BO. Figure 2 depicts the approach of the Li atom to the B-site of the BO moiety. Using valence bond-Lewis (vbl)

TABLE 2: Total Energies E (hartree), Bond Distances r_e (Å) and Angles $\theta(\angle \text{LiOB})$ (deg), Dissociation Energies D_e (kcal/mol), Dipole Moments μ (Debye), and Mulliken Charges q of the Linear Li–BO, Li–OB, and Bent Li–OB Isomers at the MRCI (2/5)^a and t-MRCI(10/12)^a Level of Theory

state	method	$-E$	$r_e(\text{B}-\text{O})$	$r_e(\text{B}-\text{Li})$	$r_e(\text{O}-\text{Li})$	θ	D_e^b	$D_e + Q^{b,c}$	μ	q_{Li}	q_{B}	q_0
linear Li-BO $X^1\Sigma^+$	(2/5)	107.40171	1.209	2.124	—	0.0	69.0	75.8	9.02	+0.30	+0.57	-0.86
	t-(10/12)	107.43031					73.5	79.9	8.90	+0.35	+0.51	-0.86
$1^1\Sigma^+$	(2/5)	107.27178	1.205	4.133	—	0.0	30.0	34.6	7.96	+0.43	+0.36	-0.79
	t-(10/12)	107.29268					29.6	31.9	7.62	+0.24	+0.48	-0.72
$^3\Pi$	(2/5)	107.24709	1.215	2.215	—	0.0	14.5	16.0	6.26	+0.37	+0.48	-0.85
	t-(10/12)	107.27236					16.9	17.7	5.83	+0.35	+0.47	-0.82
bent Li-OB \tilde{X}^1A'	(2/5)	107.40330	1.247	—	1.717	108.4	70.0	77.6	7.54	+0.41	+0.50	-0.91
	t-(10/12)	107.43118					74.1	81.9	7.55	+0.57	+0.30	-0.87
$^3A'$	(2/5)	107.30084	1.235	—	1.806	101.2	5.73	6.39	1.69	+0.24	+0.57	-0.81
	t-(10/12)	107.32294					6.15	6.40	2.73	+0.07	+0.65	-0.72
linear Li-OB $X^1\Sigma^+$	(2/5)	107.40269	1.252	—	1.664	180.0	69.6	78.1	-9.72	+0.50	+0.14	-0.64
	t-(10/12)	107.42948					73.0	82.0	-9.61	+0.54	+0.06	-0.60
$1^3\Sigma^+$	(2/5)	107.30486	1.198	—	1.923	180.0	8.24	7.81	7.57	-0.14	+0.77	-0.63
	t-(10/12)	107.32704					8.72	8.31	7.13	-0.15	+0.71	-0.56
$1^1\Sigma^+$	(2/5)	107.30180	1.199	—	1.926	180.0	48.8	49.8	7.46	-0.11	+0.78	-0.67
	t-(10/12)	107.32417					49.4	49.8	7.43	—	—	—
$^3\Pi$	(2/5)	107.28066	1.293	—	1.643	180.0	35.5	36.0	-8.44	+0.67	+0.03	-0.70
	t-(10/12)	107.30241					35.7	37.3	-7.91	+0.63	+0.03	-0.66
$^1\Pi$	(2/5)	107.24987	1.204	—	1.893	180.0	16.2	16.8	4.50	-0.17	+0.78	-0.61
	t-(10/12)	107.27272					17.1	17.3	4.34	-0.18	+0.78	-0.58
$2^3\Sigma^+$	(2/5)	107.23333	1.205	—	1.807	180.0	5.82	5.24	-5.43	-0.12	+0.71	-0.59
	t-(10/12)	107.25502					5.99	6.05	—	—	—	—
$2^1\Sigma^+$	(2/5)	107.22128	1.206	—	1.834	180.0	27.4	23.6	0.24	-0.40	+1.40	-1.00
	t-(10/12)	107.24598					28.4	18.1	-0.16	-0.37	+1.32	-0.95

^a MRCI out of CASSCF(2/5) or truncated CASSCF(10/12), see text. ^b Dissociation energies with respect to the asymptotic products. ^c D_c +Davidson correction.

diagrams, all singlets shown correspond qualitatively to the following interactions:



The three $^1\Sigma^+$ states, $X^1\Sigma^+$, $1^1\Sigma^+$, and $2^1\Sigma^+$ (Figure 2), stem from the mixing of schemes (I), (II) and (IV), i.e., $|^1\Sigma^+\rangle \approx C_1|I\rangle + C_2|II\rangle + C_4|IV\rangle$, where C_1 , C_2 , and C_4 are variational coefficients. For instance, for the $X^1\Sigma^+$ state the CASSCF(2/5) vector (C_1 , C_2 , C_4) at distances 10.0, 4.5, and 2.12 (\sim equilibrium) Å, are (0.91, 0.42, 0.00), (0.61, 0.68, -0.40), and (0.07, 0.31, -0.95), respectively. These numbers imply that the $X^1\Sigma^+$ PEC suffers an avoided crossing around 5 Å with the $1^1\Sigma^+$ state correlating to $Li(^2P; M = 0) + BO(X^2\Sigma^+)$, which has already experienced an avoided crossing at about 9 Å with the $2^1\Sigma^+$ state correlating to $Li^+ + BO^-$ fragments. From Table 2, we read that the $Li-BO(X^1\Sigma^+)$ $D_e(Li-BO) = 73.5$ kcal/mol at the t-MRCI(10/12)/MRCI(2/5) level, with an estimated Davidson corrected value of 80 kcal/mol with respect to the ground-state fragments. These values are in agreement with the results of Fuentealba.⁵

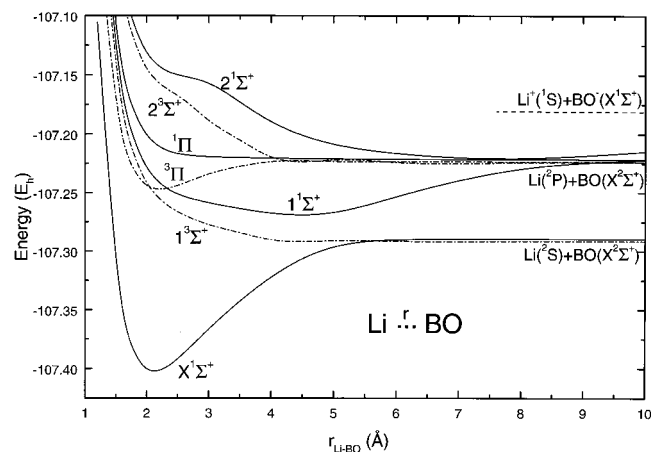


Figure 2. Singlet and triplet potential energy curves of the linear Li...BO interaction at the MRCI(2/5) level.

Around equilibrium (4 Å) the (C_1 , C_2 , C_4) coefficients for the $\mathbf{1}\Sigma^+$ state are (-0.11, 0.79, 0.61), corroborating our previous analysis. Its binding energy with respect to $\text{Li}(\text{P}; M = 0) + \text{BO}(\text{X}^2\Sigma^+)$ is $D_e(\text{Li}-\text{BO}) = 30$ kcal/mol at the t-MRCI(10/12)//MRCI(2/5) level (Table 2).

The $2^1\Sigma^+$ state correlates adiabatically to the ionic fragments $\text{Li}^+(^1\text{S}) + \text{BO}^-(\text{X}^1\Sigma^+)$, with a very flat minimum of “Coulombic” character around 8 Å due to the avoided crossing with the $1^1\Sigma^+$ state, as previously discussed. An approximate $D_e(\text{Li}-\text{BO})$ value of 30 kcal/mol is obtained at the MRCI(2/5) level.

The ${}^1\Pi$ ($\dots 4s^2 5s^2 6s^1 11\pi_x^2 1\pi_z^2, 2\pi^1$) Li-BO state correlating to $\text{Li}({}^2\text{P}; M = \pm 1) + \text{BO}(\text{X}^2\Sigma^+)$ (scheme III), is practically repulsive.

Li-OB. We discuss now the singlets due to the linear Li approach from the O-site of the BO molecule; Figure 3 shows corresponding PECs. One would expect that such an approach

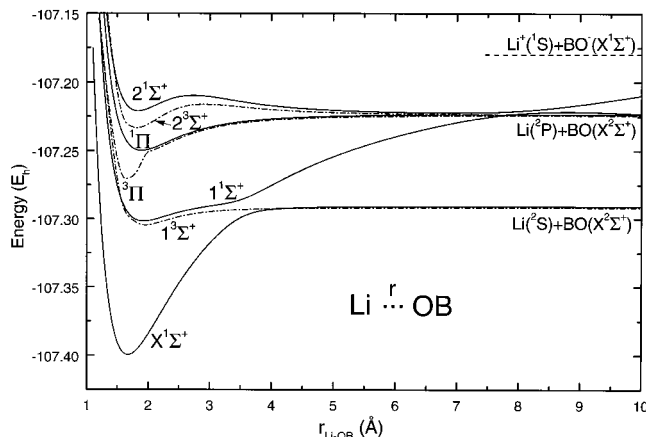
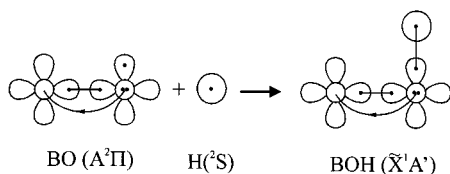


Figure 3. Singlet and triplet potential energy curves of the linear Li...OB interaction at the MRCI(2/5) level.

would lead to a repulsive Pauli interaction. On the contrary, an interactive attraction is observed leading to the strongly bound $X^1\Sigma^+$ state of the Li–OB “isomer”, Table 2. The reason is, obviously, the avoided crossing around 3.5 Å with the $1^1\Sigma^+$ state correlating to $\text{Li}(^2\text{P}; \text{M} = 0) + \text{BO}(X^2\Sigma^+)$. However, the $1^1\Sigma^+$ state has already suffered an avoided crossing at 8 Å, with the $2^1\Sigma^+$ state correlating to the ionic fragments $\text{Li}^+(^1\text{S}) + \text{BO}^-(X^1\Sigma^+)$. As a result, the $X^1\Sigma^+$ Li–OB linear state shows an intense ionic character as is also revealed by the population analysis at the t-MRCI(10/12)/MRCI(2/5) level, Table 2. This ionic character is responsible for the extreme floppiness of the Li–OB system mentioned previously (Figure 1).

The Li–OB binding energy is $D_e = 73$ (82) kcal/mol at the t-MRCI(10/12)/MRCI(2/5) (+Q) level of theory, accidentally isoenergetic with the $\text{Li}-\text{BO}(X^1\Sigma^+)$ isomer.

It is of interest at this point to mention the important difference between the Li[BO] and H[BO] isovalent systems. The latter has two nonisoenergetic isomers, one linear H–BO ($X^1\Sigma^+$) and one strongly bent H–OB ($\tilde{\chi}^1\text{A}'$; $\theta = 121^\circ$), the linear being more stable by 45 kcal/mol.^{17,18} In the H[BO] case, the linear σ -type binding is fully explained by scheme I. However, in the bent H–OB molecule, the binding entails the first excited $A^2\Pi$ state of BO, as indicated succinctly by the following valence bond Lewis diagrams (see also ref 1):

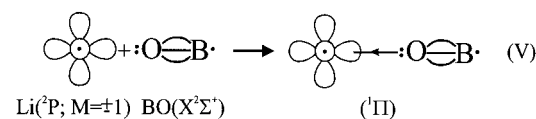


In the Li–OB case, there is competition between the $\text{Li}(^2\text{S}) + \text{BO}(\text{A}^2\Pi)$ and $\text{Li}^+(^1\text{S}) + \text{BO}^-(X^1\Sigma^+)$ reactants, almost isoenergetically located on the energy surface: $\text{BO}(X^2\Sigma^+ \leftarrow \text{A}^2\Pi) = 2.96$ eV,¹⁶ $\text{IP}(\text{Li})^{11} - \text{EA}(\text{BO})^{12} = 5.39 - 2.50 = 2.89$ eV. The ionic interaction takes over resulting finally to the $X^1\Sigma^+$ Li–OB state already discussed.

The $1^1\Sigma^+$ state presents a minimum at $r_e(\text{Li–OB}) = 1.926$ Å, with $D_e(\text{Li–OB}) = 49.4$ kcal/mol with respect to $\text{Li}(^2\text{P}; \text{M} = 0) + \text{BO}(X^2\Sigma^+)$, or 6.9 kcal/mol with respect to the ground state products (Table 2). It is interesting that the in situ Li atom is slightly negatively charged (0.11 e⁻) due to electron promotion to the $2p_z$ Li orbital.

The $1^1\Pi$ state correlates to $\text{Li}(^2\text{P}; \text{M} = \pm 1) + \text{BO}(X^2\Sigma^+)$, with $r_e(\text{Li–OB}) = 1.643$ Å and $D_e(\text{Li–OB}) = 17.1$ kcal/mol at the t-MRCI(10/12)/MRCI(2/5) level. The bonding and the in situ

negatively charged Li atom (0.18 e⁻) can be rationalized by the vBL scheme V:



The $2^1\Sigma^+$ state correlates adiabatically to $\text{Li}^+(^1\text{S}) + \text{BO}^-(X^1\Sigma^+)$, but due to an avoided crossing with the $1^1\Sigma^+$ state around 8 Å, it correlates diabatically to $\text{Li}(^2\text{P}; \text{M} = 0) + \text{BO}^-(X^2\Sigma^+)$. The observed minimum at $r_e(\text{Li–OB}) = 1.834$ Å with $D_e(\text{Li–OB}) = 28$ kcal/mol is caused instead by an avoided crossing due to an incoming (not calculated) higher $1^1\Sigma^+$ state.

4.2. Triplets. We now examine the Li–BO and Li–OB linear triplets of Σ^+ and Π symmetries (Figures 2 and 3, respectively).

Li–BO. The $1^3\Sigma^+/2^3\Sigma^+$ states correlate to $\text{Li}(^2\text{S}/^2\text{P}; \text{M} = 0) + \text{BO}(X^2\Sigma^+)$ and are purely repulsive as expected referring to schemes I and II but with the two open electrons coupled into a triplet. The 3Π state corresponds to scheme III and is characterized by a slight σ -interaction and a strong electron transfer from the Li p_π orbital to the π system of BO, giving rise to $D_e(\text{Li–BO}) = 17$ kcal/mol at $r_e(\text{Li–BO}) = 2.215$ Å (Table 2).

Li–OB. The $1^3\Sigma^+/2^3\Sigma^+$ states trace their lineage to $\text{Li}(^2\text{S}/^2\text{P}; \text{M} = 0) + \text{BO}(X^2\Sigma^+)$. Both show shallow minima with $D_e(\text{Li–BO}) = 8.7$ and 6.0 kcal/mol at $r_e(\text{Li–OB}) = 1.923$ and 1.807 Å, respectively. In the $1^3\Sigma^+$ state, the bonding is caused by a charge transfer to a $2p_z$ orbital of Li, thus rendering the Li atom slightly negative (0.15 e⁻). For the $2^3\Sigma^+$ state, the minimum is, perhaps, due to an avoided crossing with a higher $3\Sigma^+$ state, the situation being analogous to the $2^1\Sigma^+$ Li–OB state (vide supra).

The potential energy curve of the 3Π state at infinity is described by the wave function $|\text{Li}, ^2\text{P}; \text{M} = \pm 1\rangle \otimes |\text{BO}, X^2\Sigma^+\rangle$ (scheme V). The 3Π curve follows closely the $1^1\Pi$ PEC up to 2 Å; at this point, it seems to experience an avoided crossing with a higher 3Π state of strong ionic character, as the Mulliken charges indicate ($\text{Li}^{+0.65}$ at equilibrium). This higher 3Π state could stem from a 3Π BO^- state stabilized in the Coulomb field of $\text{Li}^+(^1\text{S})$.¹⁹

Finally, the $3\text{A}'$ Li–OB bent state (Table 2) with $\angle \text{LiOB} = 101.2^\circ$ and $r_e(\text{Li–OB}) = 1.806$ Å results through a partial electron transfer from $\text{Li}(^2\text{S})$ to the π -system of BO.

5. Summary and Remarks

In the present report, we have examined the interaction Li + BO using multireference methods and basis sets of quadruple quality. Our main conclusions are the following:

- The Li[BO] is a genuine polytopic system with three minima, two linear (Li–BO, Li–OB) and one bent, practically degenerate within the accuracy of our methods. Formally, the bent isomer is the global minimum ($\tilde{\chi}^1\text{A}'$) at the t-MRCI(10/12)/MRCI(2/5) level, its total energy being lower by 0.5 or 1 kcal/mol from the linear Li–BO or Li–OB $1^1\Sigma^+$ state, respectively. However, at the t-MRCI(10/12)/MRCI(2/5) + Davidson correction level, the linear Li–OB and bent Li–OB isomers are isoenergetic. According to our calculations, the Li atom can move practically freely around the O-site of BO and within a $\angle \text{LiOB}$ angle range of 100–180°.
- The two linear isomers, Li–BO and Li–OB, are separated by an energy barrier of 10.5 kcal/mol. It is of interest to note at this point that the isoelectronic Li[CN] molecule behaves similarly to Li[BO], presenting an energy isomerization barrier

Li—CN to Li—NC of about 10 kcal/mol, with the Li—NC being the stablest isomer by 6.5 kcal/mol at the SCF level.²⁰ In addition, the study of the Li[CN] dynamics has revealed interesting phenomena related to chaos,²¹ leading us to surmise that similar behavior should be expected for the Li[BO] system. c. The presence of a low-lying ionic state $\text{Li}^+\text{BO}^-({}^1\Sigma^+)$ affects strongly all states of the same symmetry, imparting finally its character to all three minima, thus explaining the ionic character of the Li[BO] system.

Acknowledgment. This work was supported by the National and Kapodistrian University of Athens through Grant 70/4/3340.

References and Notes

- (1) Papakondylis, A.; Mavridis, A. *J. Phys. Chem. A* **1999**, *103*, 9359 and references therein.
- (2) Nemukhin, A. V.; Almlöf, J. E.; Heiberg, A. *Theor. Chim. Acta* **1981**, *59*, 9.
- (3) Neubert, A. *J. Chem. Phys.* **1985**, *82*, 939.
- (4) Nemukhin, A. V.; Stepanov, N. F. *Theor. Chim. Acta* **1985**, *67*, 287.
- (5) Fuentealba, P. *Chem. Phys. Lett.* **1999**, *301*, 59.
- (6) (a) Dunning, T., Jr. *J. Chem. Phys.* **1989**, *90*, 1007. (b) Peterson, K. A.; Woon, D. E.; Dunning, T. H., Jr. *J. Chem. Phys.* **1994**, *100*, 7410.
- (7) Docken, K.; Hinze, J. *J. Chem. Phys.* **1972**, *57*, 4928. Werner, H. J.; Meyer, W. *J. Chem. Phys.* **1981**, *74*, 5794.
- (8) Werner, H.-J.; Knowles, P. J. *J. Chem. Phys.* **1988**, *89*, 5803. Knowles, P. J.; Werner, H.-J. *Chem. Phys. Lett.* **1988**, *145*, 514. Werner, H.-J.; Reinsch, E. A. *J. Chem. Phys.* **1982**, *74*, 3144. Werner, H.-J. *Adv. Chem. Phys.* **1987**, *LXIX*, 1.
- (9) MOLPRO is a package of ab initio programs written by Werner, H.-J.; Knowles, P. J., with contributions from Almlöf, J.; Amos, R. D.; Berning, A.; Deegan, M. J. O.; Eckert, F.; Elbert, S. T.; Hamble, C.; Lindh, R.; Meyer, W.; Nicklass, A.; Peterson, K.; Pitzer, R.; Stone, A. J.; Taylor, P. R.; Mura, M. E.; Pulay, P.; Schuetz, M.; Stoll, H.; Thorsteinsson, T.; Cooper, D. L.
- (10) Bunge, C. F.; Barrientos, J. A.; Bunge, A. V.; Cogordan, J. A. *Phys. Rev. A* **1992**, *46*, 3691.
- (11) Moore, C. E. *Atomic Energy Levels*; NSRDS-NBS Circular No 35; US CPO: Washington, DC, 1971.
- (12) Wenthold, P. G.; Kim, J. B.; Jones, K.-L.; Lineberger, W. C. *J. Phys. Chem. A* **1997**, *101*, 4472 and references therein.
- (13) Papakondylis, A.; Mavridis, A. *Chem. Phys. Lett.* **2001**, *341*, 382.
- (14) Langhoff, S. R.; Davidson, E. R. *Int. J. Quantum Chem.* **1974**, *8*, 61. Blomberg, M. R. A.; Sieghbahn, P. E. M. *J. Chem. Phys.* **1983**, *78*, 5682.
- (15) Tanimoto, M.; Saito, S.; Hirota, E. *J. Chem. Phys.* **1986**, *84*, 1210.
- (16) Huber, K. P.; Herzberg, G. *Molecular Spectra and Molecular Structure: IV. Constants of Diatomic Molecules*; Van Nostrand Reinhold Co: New York, 1979.
- (17) Boldyrev, A. I.; Simons, J. *J. Chem. Phys.* **1999**, *110*, 3765.
- (18) Richards, C. A.; Vacek, G.; DeLeeuw, B. J.; Yamaguchi, Y.; Schaefer, H. F., III *J. Chem. Phys.* **1995**, *102*, 1280.
- (19) For the BO^- anion, we have calculated an energy gap $a^3\Pi \leftarrow X^1\Sigma^+$ of 2.70 eV at the CCSD(T)/d-aug-cc-pV5Z level, very close to the IP = 2.50 eV of BO^- .
- (20) Essers, R.; Tennyson, J.; Wormer, P. E. S. *Chem. Phys. Lett.* **1982**, *89*, 223.
- (21) Borondo, R.; Zembekov, A. A.; Benito, R. M. *J. Chem. Phys.* **1996**, *105*, 5068.